Polymers in solution

1990 J. Phys.: Condens. Matter 2 1

(http://iopscience.iop.org/0953-8984/2/1/001)

J. Phys.: Condens. Matter. 2 (1990) 1–24. Printed in the UK

REVIEW ARTICLE

Polymers in solution

G Jannink† and J des Cloizeaux‡

† Laboratoire Léon Brillouin (Laboratoire commun CEA-CNRS), CEN-Saclay, 91191 Gif-sur-Yvette Cédex, France

‡ Service de Physique Théorique, CEN-Saclay, 91191 Gif-sur-Yvette Cédex, France

Received 24 July 1989

Abstract. We discuss the physical nature of interactions between linear flexible chains in a solvent. We review the results obtained on the structure of polymer solutions, with the help of the observation techniques and conceptual approaches developed since 1965. Comparison between observed and predicted behaviour is made for values of the critical exponents and the universal amplitude.

Table of contents

0953-8984/90/010001 + 24 $03.50

List of main symbols

a	Size of a monomer
b	Intensity of interaction between two points on a polymer chain
C	Polymer concentration
N	Number of monomers in a polymer chain
q	Momentum transfer in a scattering experiment
$^{\circ}R^2$	Average square end-to-end distance of the equivalent random walk chain
R^2	Average square end to end of the polymer chain
S	Area proportional to the degree N of polarisation. Intrinsic measure of the quantity of the polymeric material in a polymer chain ($S = {}^{\circ}R^2/3$)
X	Swelling ($= R^2/{}^{\circ}R^2$)
z	Coupling constant
$Z(S)$	Partition function of a polymer chain with one end at the origin
$Z(S, S)$	Connected partition function of two chains, one of them having a fixed end of the origin
β	$= 1/k_{\mathrm{B}}T$
π	Osmotic pressure

1. Introduction

Polymers dispersed in solvents at room temperature form polymer solutions. This is the state in which linear chains are characterised. Osmotic pressure measurements in polymer solution revealed for the first time the existence of high molecular masses and this result confirmed the macromolecular hypothesis.

In dilute solutions, the polymer chains behave, to a first approximation, as a gas. Indeed, the expression for the osmotic pressure is similar to the ideal gas law. There are, however, several intriguing facts that have aroused theoretical interest. A general and systematic interpretation has only been given recently:

(i) the chain swells in good solvents, but does not in poor solvents (i.e. in the vicinity of a 'Boyle' temperature);

(ii) the chains overlap the total solution volume, while the polymer concentration is still low.

Thermodynamic predictions based on the liquid lattice theory do not fit osmotic experimental data.

Since 1970, results of neutron scattering experiments have become available for the first time. They provided data on the structure of labelled fractions in polymer solutions. Intra- and interchain correlations could be measured separately. This information made it necessary to examine polymer solutions in more detail [1]. It became apparent that overlapping polymers do not form a homogeneous system: correlations in the structure change at a characteristic length. An inhomogeneity could thus be resolved with use of the neutron scattering technique and this gave great confidence for the investigation of closely related systems such as polymer networks.

At the same time, concepts were developed that departed radically from the liquid lattice theory. Bold modellings of polymer solutions were proposed. The history of this development is now well known. In 1972, de Gennes gave an equivalence between the partition function of a single chain and the Green function in field theory. In 1974, des

Cloizeaux showed the equivalence between polymer concentration and applied external field. However, this equivalence was first restricted to systems in equilibrium polymerisation. The other decisive innovation came from early work (1965) by S F Edwards, who introduced the path integral method to calculate observables associated with the random conformation of a polymer chain.

As shown by des Cloizeaux and later by Duplantier, the combination of these contributions proved to be very fruitful. It allowed major progress in the study of polymers and it opened up the way to original developments. A considerable number of publications have been devoted to this aspect. In particular, four books [2–5] have been written about the subject. The present paper reports established facts. It will mostly follow [4].

2. Molecular interaction: a comparison between polymers and colloids

The interaction between molecules is determined to a great degree by their structure. In particular, the compactness of the molecule plays an important role. The case of polystyrene is of interest because it is possible to polymerise this molecule in two different forms: tenuous and compact.

(i) Linear polymer chains are obtained by free radical or anionic polymerisation. When dissolved in a good solvent, the chains have a random configuration. The average volume that a chain occupies is much larger than the effective molecular partial volume.

(ii) The so-called latex spheres are obtained by emulsion polymerisation. After washing out the surfactant in a non-solvent (such as alcohol), one obtains a suspension of compact spheres. Of course, there are many other types of colloidal suspensions of hard spheres, and our system is perhaps not the best representative. However, we wish to compare comparable situations. When the spheres are dispersed in a good solvent, the chains will ultimately unfold and adopt the linear random configuration. This process takes time, and at the onset the dispersed phase is a solution of hard spheres. There are ways to stabilise the spheres permanently against dissolution, but we consider the somewhat extreme situation in which we may have a solution of stable spheres of pure polystyrene in the same solvent as linear polystyrene solutions. The samples are given the same degree of polymerisation ($N \sim 10^7$).

Our purpose is to compare the interactions between the two distinct types of high molecular structure. They will be different and we wish to point out the origin of this difference. We start from the interaction potential $v(r)$ between the two bare monomers of size a and, for simplicity, we shall assume that $v(r)$ is of the form

$$\begin{aligned} v(r) &= \infty \qquad && r < 2a \text{ (core repulsion)} \\ v(r) &= -\sigma/r^6 \qquad && r \geqslant 2a \text{ (van der Waals attraction).} \end{aligned} \tag{2.1}$$

A measure of the strength of this interaction is given by the co-volume v which is defined by

$$v = \int_0^\infty \mathrm{d}^3 r \, (1 - \mathrm{e}^{-\beta v(r)})$$

and which, for small values of σ ($\beta\sigma/(2a)^6 \ll 1$) is given by

$$v = \frac{4\pi}{3}\left((2a)^3 - \frac{\beta\sigma}{(2a)^3}\right) > 0. \tag{2.2}$$

Two cases will now be considered: the case where the monomers constitute a linear

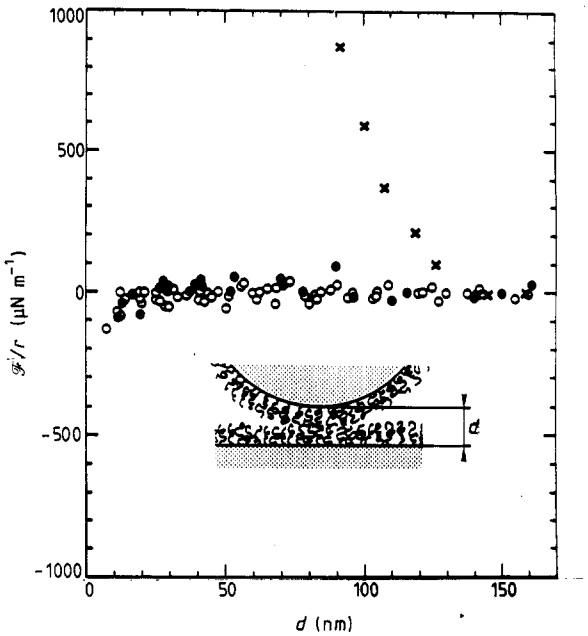

Figure 1. Forces between mica surfaces bearing terminally anchored polymer chains in good solvents, plotted against distances. ○, ● bare surfaces: the data show van der Waals attractive forces. ×, surfaces with anchored polymers: the data show repulsion between the plates. (From Taunton *et al* [6].)

flexible chain made up of N monomers, and the case where the monomers constitute a globule, also containing N monomers. For dilute solutions, the osmotic pressure π can be expanded in the form

$$\pi\beta/C = 1 + CA_2 + \ldots$$

where C is the concentration of polymerised molecules. The second virial coefficient A_2 defines the interaction between two chains in a realistic manner. This coefficient will be calculated in both cases and very different results will be obtained.

2.1. *Linear flexible chains*

For a solution of polymers with degree of polymerisation N, the second virial coefficient reads

$$A_2 = -\tfrac{1}{2}Z(N, N)/|Z(N)|^2. \tag{2.3}$$

Here, $Z(N)$ is the number of configurations of a chain with a fixed end point and $Z(N, N)$ is the connected partition function of two chains, one of them having a fixed end point. To first order (single-contact approximation) we have

$$A_2 = \tfrac{1}{2}vN^2 \simeq N^2\frac{2\pi}{3}\left((2a)^3 - \frac{\beta\sigma}{(2a)^3}\right). \tag{2.4}$$

If σ is not large, A_2 is positive. This is what is generally observed: at room temperature, the interaction between polymers in solution is usually repulsive [6] (see figure 1).

2.2. Compact spheres

When the chains form spherical globules of radius R, the interaction $V(r)$ between two spheres can be written as follows:

$$V(r) = \infty \qquad r < 2R$$

$$V(r) = V_w(r) \equiv -\left(\frac{N}{4\pi R^3/3}\right)^2 \int_{r_1<R} d^3r_1 \int_{r_2<R} d^3r_2 \frac{\sigma}{|r + r_2 - r_1|^6} \qquad r \geqslant 2R.$$

In this case, the second virial coefficient is given by

$$A_2 = \tfrac{1}{2}\int_0^\infty d^3r\,[1 - \exp(-\beta V(r))] \tag{2.5}$$

and for weak attractions

$$A_2 = \frac{2\pi}{3}(2R)^3 + \tfrac{1}{2}\int_{r>2R} d^3r\,\beta V_w(r). \tag{2.6}$$

Moreover, assuming that the globule is a compact set of small spheres of radius a, we can write

$$4\pi R^3/3 = 2^{5/2}Na^3 \tag{2.7}$$

(the volume $2^{5/2}a^3$ corresponds to a face-centred cubic arrangement), where

$$R^3 \simeq 1.350\,Na^3. \tag{2.8}$$

An exact expression for $V_w(r)$ has been given by Hamaker [7]; the result is

$$V_w(r) = -\frac{\pi^2}{6}\left(\frac{N}{4\pi R^3/3}\right)^2 \sigma\left[\frac{2R^2}{r^2 - (2R)^2} + \frac{2R^2}{r^2} + \ln\left(\frac{r^2 - (2R)^2}{r^2}\right)\right]. \tag{2.9}$$

We note that this function has two interesting limits

$$V_w(r) \simeq -N^2\frac{\sigma}{r^6} \qquad \text{for } \frac{r}{2R} \gg 1 \tag{2.10}$$

and

$$V_w(r) \simeq -\frac{3}{2}N^2\frac{\sigma}{(2R)^5}\frac{1}{r - 2R} \qquad \text{for } 0 < \frac{r - 2R}{2R} \ll 1. \tag{2.11}$$

This potential displays the Hamaker divergence [7] for $r \to 2R$. This divergence makes it necessary to introduce a cut-off at $r = 2R + a_c$, where a_c is proportional to a.

Thus, neglecting terms that vanish when $a_c/R \to 0$, we obtain

$$V_w = \int_{2R+a_c}^\infty d^3r\,V_w(r) = -6\pi\frac{N^2\sigma}{(2R)^3}\left[\ln\left(\frac{2R}{a_c}\right) - \frac{5}{3}\ln 2 - \frac{4}{3}\right].$$

Finally, for $N \gg 1$, we obtain

$$A_2 = N\frac{4\pi}{3}\left[(1.35)(2a)^3 - \frac{3}{2}\frac{\beta\sigma}{(1.35)(2a)^3}\left(\ln N + 3\ln(0.183)\frac{a}{a_c}\right)\right]. \tag{2.12}$$

Now, the existence of the factor $\ln N$ has a strong influence on the value of A_2 and if N is large enough A_2 becomes negative (compare with (2.4)). This effect is a consequence

of Hamaker's divergence. This can be seen by making the unrealistic assumption that the van der Waals forces are exerted between the centres of the globules. In this case the value of A_2 can be deduced from equation (2.2) by performing the transformation

$$a^3 \rightarrow (1.35)N a^3 \qquad \sigma \rightarrow N^2\sigma$$

which leads to the expression

$$A_2 = N\frac{4\pi}{3}\left((1.35)(2a)^3 - \frac{\beta\sigma}{(1.35)(2a)^3}\right) \tag{2.13}$$

which must be compared with (2.12).

The main difference between polymer solutions and colloidal suspensions is then the following.

(i) In solutions above the 'Boyle' temperature (usually lower than room temperature), the effective polymer interaction is repulsive. In neutral, non-polar colloidal suspensions, interactions are attractive.

(ii) The configuration of the polymer chain varies with the strength of interaction. The average shape of the configuration is the main object of theoretical and experimental investigation.

Intermediate situations between linear polymer solutions and colloidal suspensions are found in liquid membranes [8].

3. Swelling and screening

A useful model representing a polymer chain in solution is the standard continuous model. In such a model, the chain is represented by a continuous curve which obeys self-similarity. It has the fractal dimension $D = 2$ if there is no interaction between any two points, or if this interaction is moderately small.

The curve can only be drawn approximately; nevertheless, computer simulation can produce significant pictures [9] (see figure 2). The curve shown in figure 2 is a random walk with a very small step a. When this step tends to zero the limit curve is the 'Brownian' chain. It becomes impossible to draw a tangent at any of its points, and the contour length between any two points is infinite. The curvilinear coordinate of a point will be given by the area

$$s = {}^{\circ}r^2/3 \qquad 0 \leqslant s \leqslant S$$

where ${}^{\circ}r^2$ is the average square end-to-end distance between the point and one extremity of the chain ($0 \leqslant {}^{\circ}r^2 \leqslant {}^{\circ}R^2$), in the absence of interaction. In particular, S is an intrinsic measure of the number of monomers in a chain.

The repulsion, which causes self-avoidance between any two points (s', s'') will be written

$$b\delta(\boldsymbol{r}(s') - \boldsymbol{r}(s'')). \tag{3.1}$$

Here $\delta(\boldsymbol{r})$ is the three-dimensional delta function and b is the intensity of the interaction. The relation between b and v, the monomer co-volume (2.2), is approximately: $b = v/a^4$. A considerable literature is devoted to the study of the effects of repulsive ($b > 0$) interactions. The case of attractive interactions will be discussed in section 5.

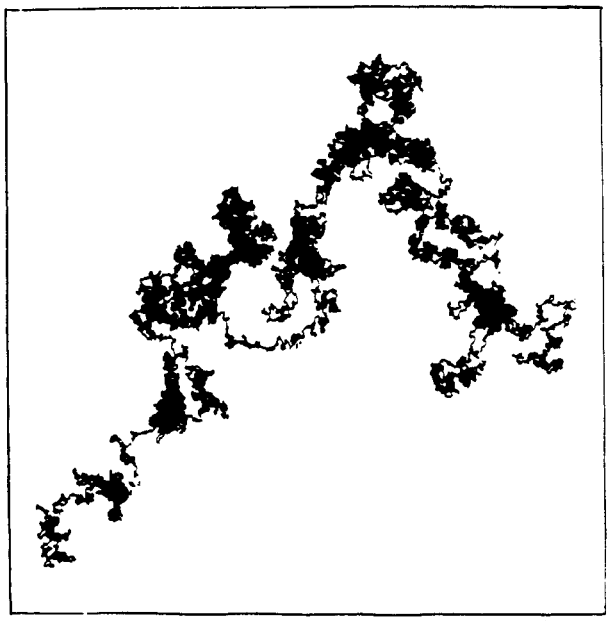

Figure 2. Two-dimensional random walk of 2×10^5 steps. (From Duplantier and Luck [9].)

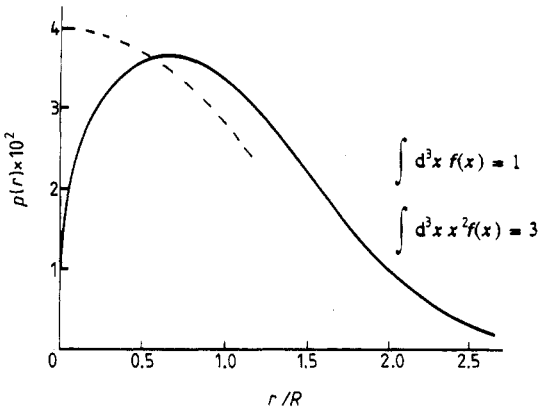

Figure 3. Density probability for the end-to-end distance of a polymer chain: ——, self-avoiding (from des Cloizeaux [10]); – – –, equivalent random walk.

3.1. The self-avoiding chain

Let us first consider the probability distribution $p(r)$ of the end-to-end distance. In the case of the random walk, $p(r)$ is a Gaussian function. When self-avoidance is introduced $p(r)$ is modified in particular at $r = 0$. Des Cloizeaux [10] showed that the perturbation at $r = 0$ extends to distances much greater than the monomer size (figure 3). In fact

$$\begin{aligned} &p(r) \propto r^{\theta} \qquad \text{for } r \to 0 \\ &\theta = 0.275. \end{aligned} \tag{3.2}$$

Computer simulations [4] confirm this prediction, but this is the only experimental evidence for (3.2). However, there exists a universal number h that accounts for the

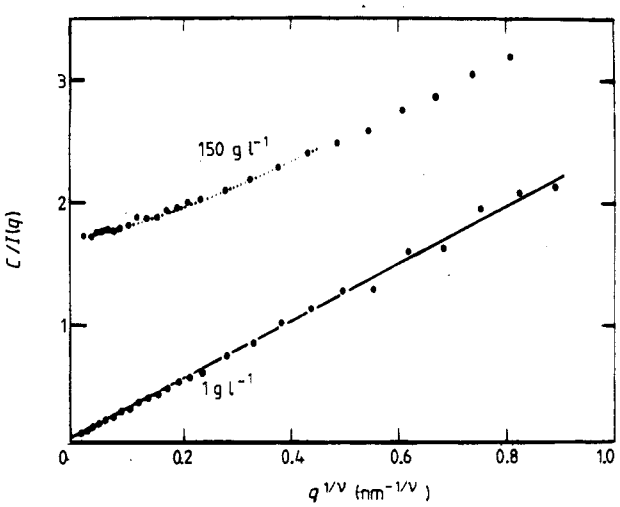

Figure 4. Inverse scattered intensities plotted against $q^{1/\nu}$. At the concentration 1 g l^{-1} the chain has a swollen configuration. The constant h is inversely proportional to the slope of the function. At the concentration 150 g l^{-1} polymer–polymer interferences become important. Swelling has decreased and screening becomes effective.

distributions $P_{ij}(r)$ of all pairs of monomers. This number has been measured. It is related to the asymptotic behaviour of the chain form function

$$h(q) = \frac{1}{S^2}\left\langle \int_d^S \mathrm{d}s' \int_d^S \mathrm{d}s'' \exp i\boldsymbol{q}\cdot(\boldsymbol{r}(s') - \boldsymbol{r}(s''))\right\rangle \tag{3.3}$$

which reads

$$h(q) \propto \frac{h}{q^2(R^2/6)^{1/2\nu}} \qquad q^2R^2 \gg 1. \tag{3.4}$$

Here ν is the critical exponent associated with the swelling of the polymer chain ($\nu = 0.588$). In the Gaussian approximation

$$^{\circ}h = 2(1/2\nu)! = 1.89 \tag{3.5}$$

but, accounting for (3.1), the value of h is smaller. From an expansion of the partition function to first order, des Cloizeaux and Duplantier [11] obtained

$$h \simeq 1.04.$$

The number h is universal. It is a measure of the density of polymer matter along the fractal path of the chain. Experimental evidence related to h is shown in figure 4. The inverse scattered intensity for scattering by a dilute polystyrene solution is plotted against momentum transfer. The value of h is determined from the slope of this function.

Recent data (absolute intensity measurement) give the result $h = 1.19$, which is in fairly good agreement with the theoretical prediction.

3.2. A characteristic geometrical constant

A characteristic quantity associated with a polymer chain is the ratio

$$R_G^2/R^2$$

of the square radius of gyration and the square end-to-end distance. For a rod, this quantity is equal to $\frac{1}{12}$, and for a random walk, $\frac{1}{6}$. In the case of a swollen chain, one expects $R_G^2/R^2 < \frac{1}{6}$. Indeed, using the Gaussian approximation, we obtain

$$R_G^2/R^2 = 1/(2\nu + 1)(2\nu + 2) = 1/6.911 \tag{3.6}$$

but a better calculation [4] gives

$$R_G^2/R^2 = 1/6.302. \tag{3.7}$$

This ratio is closer to the random walk value. The reason is the non-homogeneity of the swelling which is strongest in the centre of the chain.

3.3. Swelling of the polymer chain

Swelling of a chain results from the repulsive interaction between all pairs of monomers. The weight of a configuration is

$$\exp - b \int_0^S \mathrm{d}s' \int_0^S \mathrm{d}s'' \, \delta(\boldsymbol{r}(s') - \boldsymbol{r}(s'')). \tag{3.8}$$

After introduction of the dimensionless variable $x = s/S$, we write [12]:

$$bS^{2-(d/2)} \int_0^1 \mathrm{d}x' \int_0^1 \mathrm{d}x'' \, \delta(\boldsymbol{r}(x') - \boldsymbol{r}(x'')) \tag{3.9}$$

where d is the dimension of space. In this manner we introduce the coupling constant

$$z = bS^{2-(d/2)}(2\pi)^{-d/2}. \tag{3.10}$$

For $d < 4$, this coupling becomes infinite, as S (the size) $\to \infty$. This is the limit of interest, for which we calculate the observables. The dimension $d = 4$ is marginal (for three-body interactions, the dimension $d = 3$ is marginal). The swelling is the ratio

$$X(z) = R^2(z)/R^2(0)$$

where $R^2(z)$ is the average square end-to-end distance. This quantity diverges as $z \to \infty$. It obeys a scaling law:

$$\lim_{z \to \infty} X(z) \propto z^{2(2\nu - 1)}. \tag{3.11}$$

For available samples, $X(z)$ varies from 1 to 10. With the help of diagrams, it is possible to expand $X(z)$ in terms of the coupling constant z:

$$X(z) = 1 + \sum_{n=1}^{\infty} a_n z^n. \tag{3.12}$$

Explicit calculations of a_n were made up to $n = 6$, thus including single, double, . . . and sixfold intrachain contacts [13]. However, the series (3.12) is divergent and its radius of

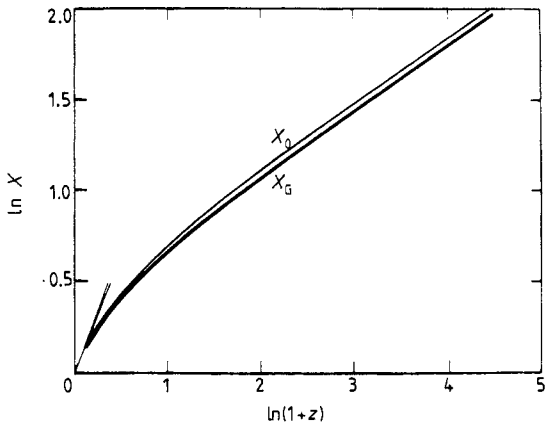

Figure 5. Calculated swellings X (end-to-end) and X_G (centre-of-mass) plotted against the coupling constant z.

convergence is zero. Des Cloizeaux *et al* [14] solved the problem by analytic renormalisation of (3.12). In this method, the swelling is expanded as a function of a characteristic number σ of the swollen state

$$\sigma = 2\nu - 1 = \tfrac{1}{2}\,\partial \ln X/\partial \ln z. \tag{3.13}$$

The quantity is *a priori* unknown, but the condition $\lim_{z\to\infty} \partial\sigma/\partial \ln z = 0$ determines $\lim_{z\to\infty} \sigma(z)$.

The expansion

$$\frac{\partial \ln X}{\partial \sigma} = \sum_{n=1}^{\infty} b_n \sigma^n \tag{3.14}$$

is calculated with the coefficients $\{a_n\}$. The final results for $X(z)$ and $\sigma(z)$ are obtained by integration of (3.14) and of $\partial \ln z/\partial\sigma$ (see figure 5). Precise experimental values of the swelling are given by light scattering data, from samples carefully prepared by fractionation.

Consistency of the model is checked by comparing theoretical and experimental values of swelling $X(S)$. Consider a set of samples i ($i = 1, 2, \ldots$ etc) characterised by different sizes S_i and experimental swellings $\bar{X}(S)$. With the help of figure 5 it is possible to determine the corresponding coupling constants z_i. We calculate the interactions

$$b_i = (2\pi)^{3/2} z_i / S_i^{1/2}. \tag{3.15}$$

If the model is consistent $b_i \equiv b$, for all samples i of a given solvent solute system, at a given temperature.

Figure 6 shows the manner in which this requirement is actually satisfied. Two sets of data [15, 16] are presented, corresponding to measurements made respectively in 1978 and 1971. The smaller dispersion of the more recent results corresponds to improved sample synthesis and data collection.

We conclude that the standard continuous model and direct renormalisation give a good account of swelling.

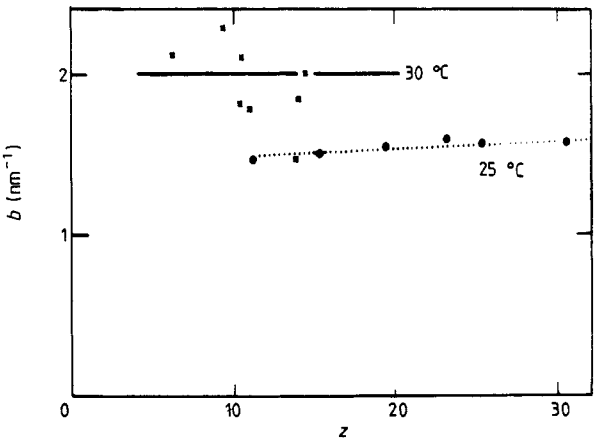

Figure 6. Interaction b derived from swelling observations and figure 5, plotted against coupling constant z. Polystyrene in benzene: ■, from Yamamoto *et al* [16]; ●, from Miyaki *et al* [15].

3.4. Osmotic coefficient and universal interaction constant

The repulsive interaction between two polymer chains determines the second virial coefficient of the osmotic pressure expansion. By definition, this coefficient is equal to the ratio of the partition functions (see (2.3)):

$$Z(S, S)/(Z(S))^2. \tag{3.16}$$

The ratio (3.16) has the dimensions of a volume. It accounts for all two-body interactions between two polymer chains in solution. Since the chains expand as an effect of the interaction, an intrinsic measure of the two chains interaction is the quantity (3.16) *per unit volume*, i.e. the number

$$g(z) = -\left(\frac{3}{2\pi}\right)^{3/2} \frac{Z(S, S)}{[Z(S)]^2} \frac{1}{(R^2)^{3/2}}. \tag{3.17}$$

This is the osmotic coefficient.

To first order in the interaction b, one has [4] (see also (2.4))

$$g(z) \simeq (2\pi)^{-3/2} bS^2/S^{3/2} = z \tag{3.18}$$

which is a result that is expected for weak interactions. The characteristic polymer property is related to the asymptotic behaviour of $g(z)$. Interaction becomes shielded as $z \to \infty$. Moreover,

$$\lim_{z\to\infty} g(z) = g^* \ (\simeq 0.233) \tag{3.19}$$

is a universal number. The fact that g^* is finite can be proved by the following argument (des Cloizeaux [4]). First, we note in (3.11) and figure 5 that the swelling $X = R^2/{}^\circ R^2$ tends to infinity as $z \to \infty$.

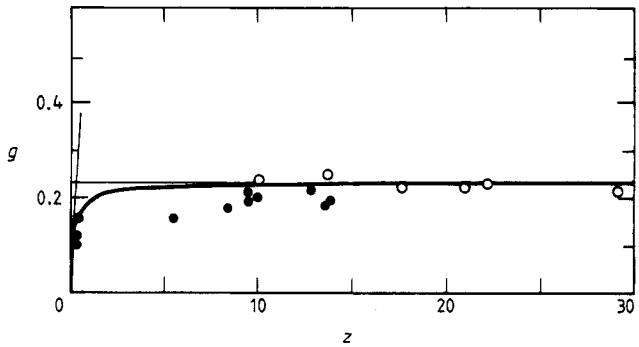

Figure 7. Osmotic coefficient g plotted against coupling constant z: ———, theoretical prediction; ○, ●, measured values. (From des Cloizeaux and Jannink [4].)

However, we may keep the square end-to-end distance, R^2, fixed, while z and $X(z)$ tend to infinity. For this, we set $S\ (=\circ R^2/3) \to 0$. This is compatible with an infinite value of

$$z = (2\pi)^{-d/2} b S^{2-(d/2)}$$

if the interaction b increases quickly enough. We now express all terms in (3.17) as a function of R^2, the size of the swollen chain, instead of $S = \circ R^2/3$. The renormalised terms are finite whatever the value of z, and this proves the assertion.

Theoretical and experimental values of $g(z)$ are shown in figure 7. The approximate expression of g^* to second order in $4 - d$ is (for $d = 3$) [4]

$$g^* = \tfrac{1}{8} + \tfrac{1}{16}(\tfrac{25}{16} + \ln 2). \tag{3.20}$$

An analogy for the osmotic coefficient g is obtained in field theory by normalisation of the four-point vertex function. In the n-vector model, the so-called 'renormalised coupling constant' u is, to second order in $4 - d$ (for $d = 3$), [17]

$$u^* = [6/(n+8)][\tfrac{1}{2} + 3(3n+14)/(n+8)^2] \tag{3.21}$$

but there is no simple relation between u^* and g^*.

3.5. *Screening in semi-dilute solutions*

In dilute solutions, the chains are far apart on average. When the polymer concentration C increases, there exists a concentration C^* at which the chains begin to overlap. This is the onset of the semi-dilute regime. We may write

$$C^* \propto 1/(R^2)^{3/2} \tag{3.22}$$

where R^2 is the square end-to-end distance at *zero* concentration.

The concentration C^* can be very low if the chains are long. Indeed, in the limit of infinitely long chains, $C^* = 0$. Thus a given concentration interval ΔC can either belong to the dilute or to the semi-dilute regime, depending on the length of the chain. The main difference between a dilute and a semi-dilute polymer concerns the homogeneity of the polymer distribution in space. Homogeneity is a discriminating factor for the effects of repulsive interaction. Dilute solutions have a heterogeneous structure: the

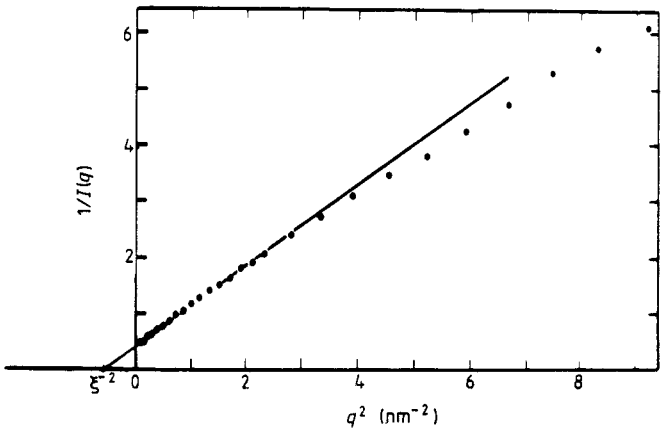

Figure 8. Inverse scattered intensity plotted against q^2 (the squared wavevector transfer). Polystyrene in CS_2. ———, formula (3.23). ●, measured values. ξ^{-2} is measured by extrapolation of the straight line. Departure from (3.23) reveals the blob structure of the solute. (From des Cloizeaux and Jannink [4].)

polymer chains form isolated islands in the solvent. The repulsive interactions between monomers add up to swell the chains.

Solutions with overlap (semi-dilute) possess a homogeneous structure on the large scale ($\sim R$). However, in between nearest neighbour contacts, the solution is dilute, and therefore inhomogeneous. The repulsive interactions acting on the homogeneous structure do not combine to swell the structure. On the contrary, compensations occur and on average the interactions *screen* the pair correlation function (figure 8). This means that correlations between monomers are effectively weaker than those associated with a random walk. Screening in polymer solutions was introduced by Edwards [18] and proved to be a unifying concept. In semi-dilute solutions, screening and swelling coexist, at different scales. This generates a structure. Chain sequences swell only within distances ξ, the screening length. This length depends on monomer concentration and interaction strength b (it is independent of polymer size).

Let us consider the experimental evidence for screening. The scattered intensity $I(q)$ (figure 8) obeys the relation

$$C/I(q) = A(q^2 + \xi^{-2}) \tag{3.23}$$

where A is a constant. The singularity $q^2 = -\xi^{-2}$ implies screening in real space, i.e. an attenuation factor $e^{-r/\xi}$. The semi-dilute regime exists in the limit of infinite chains, since the singularity is independent of chain size.

Because screening and swelling coexist, the length ξ varies in a singular manner with concentration. This is based on the following remarks.

(i) An intrinsic measure of the monomer concentration is the 'Kuhnian' concentration [3]

$$C_K = C(R^2/3)^{1/2\nu} \qquad \text{(dimension } L^{1/\nu - d}\text{)}. \tag{3.24}$$

This concentration defines the 'Kuhnian' overlap length [3]

$$\xi_K = C_K^{-1/(d-1/\nu)}. \tag{3.25}$$

(ii) The screening length ξ is proportional to ξ_K

$$\xi = \Gamma \xi_K \tag{3.26}$$

where Γ is a universal constant approximated by the relation [4]

$$\Gamma = (1/4\pi)(g^*)^{-1/2} = 0.165 \tag{3.27}$$

derived from the simple tree approximation of the structure function.

Experimental values of ξ are obtained from the scattered intensity data $I(q)$ and formula (3.23). The values of ξ derived in this manner satisfy relation (3.26). The experimental value of Γ is found to be $\Gamma = 0.18 \pm 0.015$ [4]. Formula (3.23) is quite general, but relation (3.26) between ξ^{-2} and the concentration is not trivial. It is of interest to note that the intensity scattered by a copolymer melt undergoing chain scission and recombination (polycondensation) is represented [19] by a formula similar to (3.23). Here, the screening is only a manifestation of chemical homogeneity. The case of a swollen polymer network is also of interest [20]. The distribution of the network function has a characteristic inhomogeneity which causes an excess scattering with respect to (3.23).

4. Crossover effects

The universal constants related to polymer chain structure (ν, g^*, h etc) are derived in the limit of infinite coupling constant, $z \to \infty$. However, physical chains are finite, and for instance the maximum value of z for available samples is $z \simeq 40$. Thus real chains are in a crossover state. There are many crossover situations, depending on the chain environment. The parameters associated with environment are, for instance, solution temperature, polymer concentration and molecular mass dispersion. The effect of a change in these parameters reveals the physical nature of polymer systems, even though universality is not reached.

4.1. Osmotic pressure in dilute and semi-dilute solutions

The osmotic pressure experiment provides a crucial test for polymer theory. However, it is only recently that an adequate theoretical framework has been proposed [21]. The earlier approach consisted in calculating the virial expansion in the single-contact approximation

$$\pi\beta = \sum_{n=1}^{\infty} A_n(z, {}^\circ R^2) C^n. \tag{4.1}$$

However, when such a formula fits the data in the dilute regime, it gives pressures that are too high when extrapolated in the semi-dilute regime. It fails to account for the depletion effect [2] caused by the repulsive interaction around each monomer.

The difficulty can be overcome if the fundamental length giving the scale of the system is changed from $({}^\circ R^2)^{1/2}$ to $(R^2)^{1/2}$ (R^2 is the average square end-to-end distance of the swollen chain ($C \to 0$, $z \gg 1$), whereas ${}^\circ R^2$ is the average square end-to-end

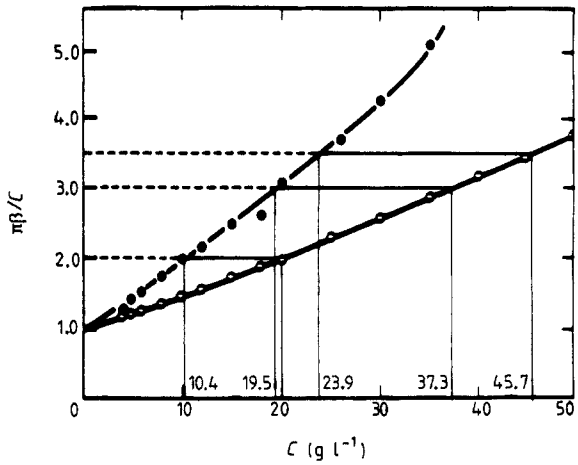

Figure 9. Reduced osmotic pressure plotted against monomer concentration: ●, polystyrene (M_w = 72 000) in toluene at 37 °C; ○, polystyrene (M_w = 155 000) in benzene at 30 °C. The horizontal and vertical lines help in checking universality. (From des Cloizeaux and Jannink [4].)

distance of the equivalent random walk). This is the direct renormalisation method [4]. This gives the result

$$\pi\beta = \sum_{n=1}^{\infty} B_n(g(z), R^2)C^n. \tag{4.2}$$

This formula contains three parameters. Since, however, $g(z)$ is practically equal to g^* for $z \geqslant 4$ (see figure 7), the osmotic pressure is a function of only two variables: the polymer concentration C and the size R^2 ($C \to 0$). We propose to test the direct renormalisation procedure on experimental data. In this manner, we shall obtain a universal representation of the osmotic pressure in good solvents [4].

Figure 9 shows two sets of osmotic pressure data, respectively for polystyrene (molecular mass 7.2×10^4) in toluene and polystyrene (molecular mass 15.5×10^4) in benzene [22]. The two curves are seen to be affine: this means that renormalisation of the concentrations by a factor 1.92 for the higher curve leads to superposition of the two curves. The renormalisation factor is equal to the ratio of the corresponding volumes $(R^2)^{3/2}$ representing the volume occupied by the chains in the limit of zero concentration. Hence, osmotic pressure data for all good solutions in the dilute and semi-dilute regime can be represented on a universal curve:

$$\pi\beta/C = F(C/C^*) \tag{4.3}$$

where C^* is given by (3.22). The asymtotic form is

$$F_\infty (3.97\ C/C^*)^{1/(\nu d - 1)}$$

where F_∞ is a universal constant ($F_\infty = 0.4855$) [4].

4.2. Crossover to concentrated solutions

The standard continuous model represents the polymer chain by an immaterial curve, as shown in figure 2. In this model, the chain occupies a certain volume $(R^2)^{3/2}$ in space,

but it has *no volume* by itself. The significative parameter is the fraction of occupied volume $C(R^2)^{3/2} = C/C^*$ (see (3.22)). The increase of the osmotic pressure associated with an increase of concentration is caused by repulsive interaction between fractal objects. The partial volume of the chain does not contribute in any way. One could imagine that this situation persists whatever the amount of polymer material filling a given volume. However, this is not the case, and beyond a certain concentration (20% by weight), the finite volume of the physical chain begins to be more significant than the overlap ratio. This is the crossover from semi-dilute to concentrated solutions. In the concentrated regime, the polymer solution behaves more like a binary liquid mixture. The osmotic pressure can now be written as

$$\pi\beta/C = G(\varphi)$$

where φ is the volume fraction of the chain. The function G has been calculated by Flory and Huggins [4]. The relation between volume fraction φ and chain overlap C/C^* is

$$\varphi = (C/C^*)C^*\mathcal{V} \simeq (C/C^*)S^{1-\nu d} \tag{4.4}$$

where $\mathcal{V}$ is the chain partial volume. Given the value of C/C^* $(=C(R^2)^{3/2})$ the volume fraction is obviously a decreasing function of the chain length.

The crossover between semi-dilute and concentrated solutions is illustrated in figure 10. The osmotic pressure is plotted against chain overlap C/C^*. In the universal regime (dilute and semi-dilute concentration) all data fit the universal curve. However, beyond a given overlap $(C/C^*)_c$ small chains give a higher osmotic pressure than long chains [23]. This is the indication of the crossover to the liquid mixture behaviour.

4.3. Bi-disperse polymer systems

A mixture of chains having two different lengths, but identical chemical nature, form bi-disperse polymer systems. These systems present interesting structural problems, which have not yet been entirely solved. Application of field theory and of renormalisation gives the answer, but some work remains to be done.

4.3.1. Swelling of a long chain in a liquid of shorter chains. Here we report predictions and observations on the swelling of a long chain in a liquid of smaller chains. The result displays interesting scale invariant properties of polymer chains.

Let S_1 be the Brownian size of the long chain, and the S the Brownian size of the shorter chains ($S \leqslant S_1$). If S is negligible with respect to S_1, the S_1-chain will swell as described in section 3.2. On the other hand, if S is of the order of S_1, the correlations are totally screened and the S_1-chain has a random walk configuration (Brownian chain). The problem is to determine the crossover function for the average swelling of the long chain $X(S_1, S)$.

For this, we express the swelling as a function of an effective coupling constant z_{eff} [4]:

$$z_{\text{eff}} = (2\pi)^{-3/2} b_{\text{eff}} S_1^{-1/2} \tag{4.5}$$

where the interaction b_{eff} is given by

$$b_{\text{eff}} = 1/CS^2. \tag{4.6}$$

Here C is the concentration of the small chains (polymer melt). Formula (4.6) is

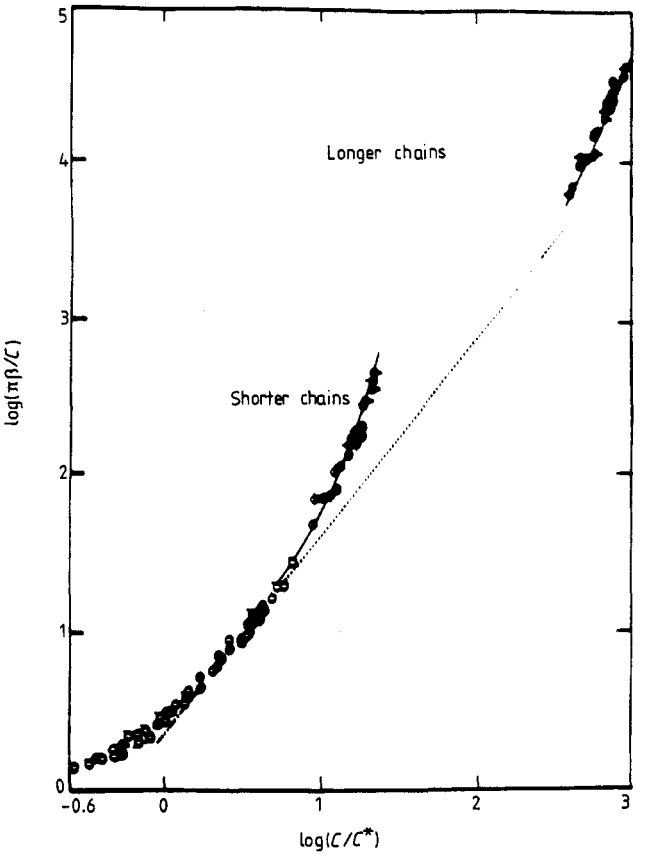

Figure 10. Reduced osmotic pressure plotted against overlap ratio: ----, calculated asymptotic form of the universal behaviour. Deviations from universality are seen at higher concentrations, at which the liquid lattice theory holds true. (From Noda *et al* [23].)

derived from the expression for the second virial coefficient for labelled chains in a homogeneous polymer melt [1]. Finally

$$z_{\text{eff}} = (2\pi)^{-3/2}(S_1/S)/CS \tag{4.7}$$

and

$$X(S_1,S) = z_{\text{eff}}^{2(2\nu-1)} \tag{4.8}$$

which is the desired result.

The quantity CS is equal to the monomer concentration. In the liquid state, this quantity is independent of the size S of the chains.

Thus $z_{\text{eff}} \sim S_1^{1/2}/S$. This is verified experimentally [24].

Let us now consider the consequences of (4.7) with respect to scale changes. If, for instance, we double both sizes S_1 and S, then z_{eff} decreases and so does the swelling X of the long chain (see figure 11). If, on the contrary, space is dilated

$$x' = \lambda x \tag{4.9}$$

then z_{eff} remains unchanged! (This is because the density of the polymer liquid changes.)

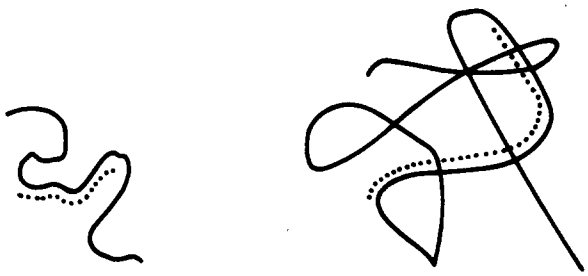

Figure 11. Schematic drawings of a long chain in a liquid of smaller chains. From left to right, the lengths of the long and smaller chains are multiplied by a factor of four. Swelling is, however, greater on the left than on the right.

4.3.2. The second virial coefficient in bi-disperse polymer solutions. The second virial coefficient of two identical chains $Z(S,S)/(Z(S))^2$ relates to the volume $(R^2)^{3/2}$ occupied by the polymer chain (3.18). It is therefore tempting to introduce the concept of equivalent impenetrable spheres. The spatial distribution of two chains would be similar to that of two rigid spheres. We have already seen that this picture is basically misleading (see section 2), but here we give another illustration of this fact. Consider the extreme case of a long chain S_1 and a short chain S, the latter being of the size of a solvent molecule. Obviously, the short chain is able to approach the long chain well inside the sphere of radius $(R^2(S_1))^{1/2}$. Thus, the equivalent hard sphere model breaks down. Witten and Prentis [25] proposed a crossover formula

$$\frac{Z(S_1,S)}{Z(S_1)Z(S)} = -\left(\frac{2\pi}{3}\right)^{3/2}\frac{S_1}{S}(R^2(S))^{3/2}\bar{g} \tag{4.10}$$

where the osmotic coefficient $\bar{g}$ is slightly smaller than g^* ($\bar{g} \simeq 0.78g^*$). Experimental results [26] seem to agree with (4.10). A good theory could give a more precise description of the polymer structure.

5. Polymer chains in poor solvents

In poor solvents, the attractive forces acting on polymer chains become important. These forces cause two observable phenomena, which are critical demixtion and chain collapse. In the standard continuous model, the balance (2.1) between repulsion and attraction is replaced by a combination of attractive two-body and repulsive three-body short range interactions.

5.1. Universality of critical demixtion?

If the temperature of a polymer solution in a poor solvent is lowered, the solution phase separates into two phases. The transformation is associated with a critical phenomenon, in the vicinity of a temperature T_c and a concentration C_c. Critical opalescence is observed. This behaviour is well described by the n-vector model, with a value $n = 1$ for the dimension of the order parameter.

The critical exponents associated with demixtion ($n = 1$, $d = 3$) are well known and their values have been verified experimentally. They are same as those measured in the demixtion of simple binary liquids. The difference concerns the domain of the temperature-concentration diagram in which observables obey the critical scaling laws. This domain is known to be quite extensive for the case of simple binary liquids. It reduces to $1/\sqrt{N}$ in the case of polymer solution, and it shrinks to an insignificant size in the case of polymer blends.

A complication arises from the fact that polymer chains in solution form by themselves a critical system in the limit $S \to \infty$. This system was recognised to belong to the n-vector model ($n = 0$, $d = 3$) [2]. Thus two critical phenomena coexist in polymer solutions and extert mutual effects on each other. In particular, in the limit $S \to \infty$ the temperature T_c tends to the Flory temperature, identified as the tricritical point [2]. Here we report an effect of the chain size S on the critical demixtion curve.

In the vicinity of critical demixtion (T_c, C_c) the solute volume fractions $\varphi'(T)$, $\varphi''(T)$ for the demixtion curve obey the scaling relation

$$(\varphi'(T) - \varphi''(T))/\varphi_c = B_a(-t)^{\beta} \tag{5.1}$$

where the reduced temperature $t = (T - T_c)/T$ is the relevant parameter; B_a is a non-universal amplitude and β is the critical exponent of the ($n = 1$, $d = 3$) model ($\beta = 0.325 \pm 0.002$). Dobashi *et al* [27] have made precise measurements of β and B_a for different polymer sizes S. They found that B_a decreases with S while β remains constant. This is the way the two critical phenomena coexist.

It has been suggested [4] that there is a better representation of the demixtion fluctuation in polymer solutions—namely, the use of a more intrinsic reduced temperature

$$\tau = (1/T_c - 1/T)/(1/T_c - 1/T_F) \tag{5.2}$$

where the result $T_F = \lim_{S\to\infty} T_c$ allows us to write

$$(\varphi'(T) - \varphi''(T))/\varphi_c = B(-\tau)^{\beta} \tag{5.3}$$

where B could be a universal amplitude. A calculation of B in the simple tree approximation gives $B = 4.9$.

Figure 12 shows the experimental results corresponding to three samples of different sizes S. In the representation (5.3) the data are seen to superpose on a unique curve. The experimental value of B is 3.7. This presentation could be useful for investigating the tricritical limit, $S \to \infty$.

5.2. Remark on chain collapse

Adam and Delsanti, using light scattering, have shown that polymer chains collapse in very dilute solutions, as the temperature is lowered towards the coexistence curve [4]. This situation presents interesting problems concerning the stability of a chain configuration at a given temperature of the solution [28].

The origin of the attractive forces that cause this collapse is related to van der Waals forces (see §2). However, Edwards and Muthukumar [29] have shown recently that effective attractive forces exist for other reasons. Namely, 'if the random walk encounters randomly placed obstacles it will localize'. Therefore, the roughness of a surface on which a polymer chain is deposited could cause collapse.

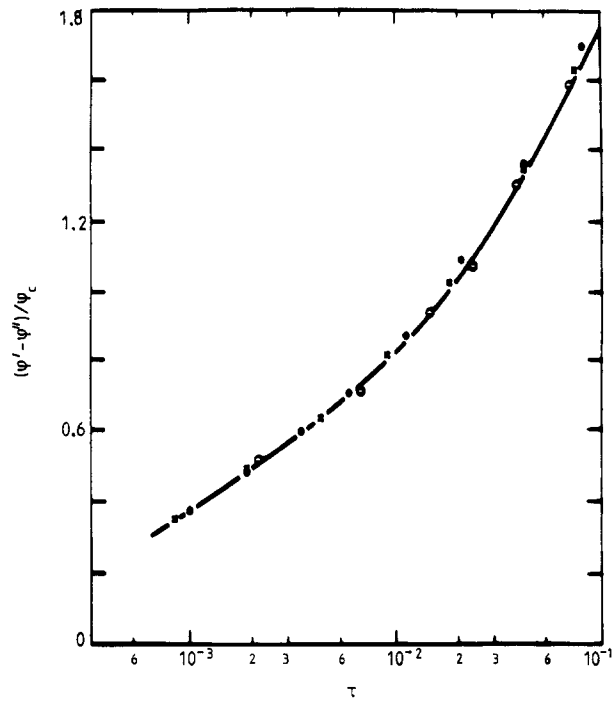

Figure 12. Universal plot of $(\varphi'(\tau) - \varphi''(\tau))/\varphi_c$ against reduced temperature τ. Polystyrene in methylcyclohexane. ○, $M_w = 1.73 \times 10^4$; ●, $M_w = 1.09 \times 10^5$; ×, $M_w = 7.19 \times 10^6$. (From des Cloizeaux and Jannink [4] and Dobashi *et al* [27].)

Another situation of interest with respect to the onset of attractive forces was predicted by de Gennes [30] (see also Brochard and de Gennes [31]). Consider a dilute polymer solution, in a mixture of two *good* solvents, which are close to their critical demixtion point. The structure of such a solvent mixture is characterised by inhomogeneities of size ξ, diverging at the critical demixtion point. For $a < \xi < R$ (where a is the monomer size and R the polymer end-to-end distance), the effective forces acting on the polymer chain are attractive. This results from the preferential solvation of a monomer for one of the solvents. As a consequence, monomers will tend to aggregate in the domains that are richer in the preferred solvent. However, it is necessary that $\xi < R$; otherwise repulsion is dominant. The authors quoted above determined a characteristic contour of the miscibility range in which the polymer chain is predicted to collapse.

5.3. Polymer solutions under shear

When shear is applied to a polymer solution, turbidity and opalescence appear at temperatures far above the stagnant cloud point. Rangel-Nafaile and co-workers [32] provided data for this observation, using polystyrene ($M_w = 8 \times 10^6$) solutions in dioctylphthalate. In their experiment, the solution is pushed through a capillary tube at a given flow rate Q. A visible cloudiness is detected at a temperature $T_c(Q)$. The results

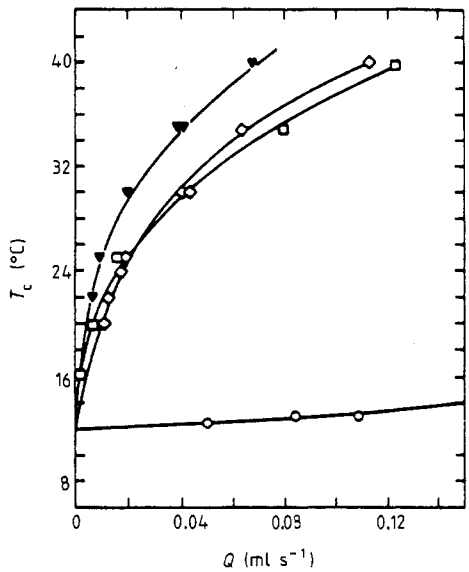

Figure 13. Plot of the cloud point temperature T_c against flow rate Q, for different concentrations of the polymer solution. (From Rangel-Nafaile *et al* [32].) ○, $C = 0.02$ g ml^{-1}; ◇, $C = 0.042$ g ml^{-1}; ▼, $C = 0.057$ g ml^{-1}; □, $C = 0.077$ g ml^{-1}.

are shown in figure 13. The effect is particularly important in semi-dilute solutions. This phenomenon is typical of the polymer solution state. It does not show in binary mixtures of simple liquids under shear.

Because the overlapping chains form a temporary network, it is natural to consider the elastic energy E of conformation stored in the solute under shear flow. This energy is proportional to the normal stress difference. When one introduces E as an external field in the expression of the solution free energy, one is able to calculate [33] cloud temperatures. A qualitative agreement with observations is obtained.

However it has been suggested [34] that it is not necessary to invoke a 'symmetry-breaking transition' to explain the observed turbidity. The flow field provides conditions for the growth of concentration waves by dissipation.

It should also be noted that bi-disperse polymer melts display [35] anomalous structure patterns when subjected to a uniaxial step strain. In reciprocal space, these patterns appear as 'butterflies'. Different interpretations are proposed for this observation, among which enhancement [36] of demixtion between short and long chains is one.

6. Conclusion

We have reported recent progress in the study of polymer solutions. Let us now summarise the results and comment on the present situation.

We have been concerned with the universal properties related to the structure of polymer solutions. Precise predictions have been obtained from the standard continuous model of the polymer chain. A typical result is the coupling constant in good solutions, or osmotic coefficient g^*, a universal number independent of the particular core repulsion and van der Waals attraction between monomers. Other characteristic numbers

Table 1. Universal constants related to polymer solutions in three dimensions [4].

Constant	Definition	Theoretical evaluation	Experimental result
$\nu(n=0)$	Swelling exponent	0.5885 ± 0.0025	Light scattering 0.588 ± 0.003
$\gamma(n=0)$	Attrition exponent	1.160 ± 0.004	Computer simulation 1.1663 ± 0.0003
θ	Contact exponent	0.275 ± 0.002	
$\nu(n=1)$	Correlation exponent	0.63 ± 0.0008	Light scattering 0.63 ± 0.005
$\beta(n=1)$	Coexistence exponent	0.325 ± 0.002	0.325 ± 0.01
h	Ratio related to the asymptotic form function	1.04	Neutron scattering 1.16
g	Osmotic coefficient	0.233	Osmotic pressure and scattering light 0.233 ± 0.007
χ	Geometrical ratio	0.952	Computer simulation 0.93
F_∞	Ratio related to osmotic pressure in the semi-diluted limit	2.467	Osmotic pressure 2.46 ± 0.02
Γ	Ratio related to screening	0.165	Neutron scattering 0.19 ± 0.01
$\mathcal{A}$	Ratio related to chain size in semi-dilute solutions	0.48	0.49 ± 0.03
B	Amplitude associated with critical demixtion	4.9	Direct observation of phase separation 3.7

Table 2. Table of universal constants related to polymer solutions in two dimensions [4].

Constant	Definition	Theoretical evaluation	Experimental result
$\nu(n=0)$	Swelling exponent	0.75	Osmotic pressure 0.79 ± 0.01
$\gamma(n=0)$	Attrition exponent	1.333	Computer simulation 1.33 ± 0.003
ν_t	Swelling exponent (tricritical)	0.55 ± 0.01	Osmotic pressure 0.56 ± 0.01
θ	Contact exponent	0.444	Computer simulation 0.49 ± 0.06
χ	Geometrical ratio	0.799	Computer simulation 0.84

attesting to the universal nature of dilute and semi-dilute polymer solutions are displayed in table 1, for three dimensions, and in table 2 for two dimensions. Thus, besides critical opalescence, polymer solutions display an intrinsic critical behaviour, corresponding to the limit of infinite chains. Tricritical and mean field behaviours are also identified.

Predictions have been tested for physical experiments and computer experiments. These experiments are complementary. However, the laws concerning the partition function and directly related quantities have only been tested by computer experiments. It is worth pointing out that new observation techniques have been developed. The isotopic substitution method, associated with the neutron scattering technique, has improved our ability to establish contrasts. The contrast between a polymer chain and its environment is at the heart of the problem, because of the fractal nature of the polymer configurations. It is also well suited for determining interaction parameters.

The standard continuous model could be used further to derive exact results, in closely related domains such as:

(i) the structure of multicomponent solutions (more than one solute or solvent);

(ii) the dynamics of polymer chains in solution. Introducing the equivalent Brownian area s (section 3.1) in the Rouse equation, one obtains immediately an expression of the internal 'diffusion' coefficient $\mathcal{D}$ in units of s^2/t ($cm^4\ s^{-1}$), which is the expected result.

Remarkably, the simple tree approximation gives good results when applied to the determination of structure functions in concentrated solutions. In semi-dilute and dilute solutions, the contribution of loops is important and explicit results need to be calculated.

The new concepts that were successfully developed for the study of linear flexible chains in solution are also applicable to other similar systems: branched polymers, gels and all sorts of finely divided matter with long range correlations. The polydispersion in these systems is an essential factor in their structure and not simply a corrigible effect.

A basically different approach is probably needed for studying systems in which the persistence length is important, such as solutions of charged molecules and, in general, mesomorph polymers.

Acknowledgments

The authors thank M Daoud and J Teixeira for criticism of the manuscript. One of us (GJ) gratefully acknowledges earlier collaboration with the STRASACOL group (Strasbourg, Saclay and College de France).

References

[1] Daoud M, Cotton J P, Farnoux B, Jannink G, Sarma G, Benoît H, Duplessix R, Picot C and de Gennes P G 1975 *Macromolecules* **8** 804
See also
Cotton J P 1973 *Thesis* Paris University
Farnoux B 1975 *Thesis* Strasbourg University
Daoud D 1977 *Thesis* Paris University
Rawiso M 1987 *Thesis* Strasbourg University
[2] de Gennes P G 1979 *Scaling Concepts in Polymer Physics* (Ithaca, NY: Cornell University Press)
[3] Doï M and Edwards S F 1986 *The Theory of Polymer Dynamics* (Oxford: Clarendon)
[4] des Cloizeaux J and Jannink G 1987 *Les Polymères en Solution; leur Modélisation et leur Structure* (Les Ulis: Editions de Physique)
[5] Freed K F 1987 *Renormalisation Group Theory of Macromolecules* (New York: Wiley)
[6] Taunton H J, Toprakcioglu C, Fetters L and Klein J 1985 *Nature* **332** 712
[7] Israelachvili J N 1985 *Intermolecular and Surface Forces* (London: Academic)
[8] Peliti L and Leibler S 1985 *Phys. Rev. Lett.* **54** 1690

[9] Duplantier B and Luck J M 1988 Saclay
[10] des Cloizeaux J 1974 *Phys. Rev.* A **10** 1665
[11] des Cloizeaux and Duplantier B 1985 *J. Physique Lett.* **46** L457
[12] Duplantier B 1988 *J. Ann. Soc. Math. France* (ed Société de Mathématiques de France, Paris)
[13] Muthukumar M and Nickel B G 1984 *J. Chem. Phys.* **80** 5839
[14] des Cloizeaux J, Conte R and Jannink G 1985 *J. Physique Lett.* **46** L595
[15] Miyaki Y, Einaga Y and Fujita H 1978 *Macromolecules* **11** 1180
[16] Yamamoto A, Fuji M, Tanaka G and Yamakawa H 1971 *Polym. J.* **2** 799
[17] Brézin E, Le Guillou J C and Zinn-Justin J 1976 *Field Theoretical Approach to Critical Phenomena in Phase Transitions and Critical Phenomena* vol 6 ed C Domb and M S Green (New York: Wiley)
[18] Edwards S F 1965 *Proc. Phys. Soc.* **85** 613
[19] Benoit H, Fisher E W and Zachmann 1989 *Polymer* **30** 379
[20] Bastide J, Leibler L and Prost J to be published
[21] des Cloizeaux J 1975 *J. Physique* **36** 281
[22] Noda I, Kato N, Kitano T and Nagasawa M 1981 *Macromolecules* **14** 668
[23] Noda I, Higo Y, Ueno N and Fujimoto T 1984 *Macromolecules* **17** 1055
[24] Kiste R G and Lehnen B R 1976 *Makromol. Chem.* **177** 1137
[25] Witten T A and Prentis J J 1982 *J. Chem. Phys.* **77** 4247
[26] Lapp A 1987 *Thesis* Strasbourg University
Broseta D 1987 *Thesis* Paris University
[27] Dobashi T, Nakata M and Kaneto M 1980 *J. Chem. Phys.* **72** 6685
[28] Benoit H, Borsali R and Duval M *Macromolecules* to appear
[29] Edwards S F and Muthukumar M 1988 *J. Chem. Phys.* **89** 2435
Edwards S F and Chen Y 1988 *J. Phys. A: Math. Gen.* **13** 2963
[30] de Gennes P G 1976 *J. Physique* **37** 59
[31] Brochard F and de Gennes P G 1980 *Ferroelectrics* **30** 33
[32] Rangel-Nafaile C, Metzner A B and Wissbrun K F 1984 *Macromolecules* **17** 1187
[33] Onuki A 1989 *Phys. Rev. Lett.* **62** 2472
[34] Helfand E and Fredicksen G H 1989 *Phys. Rev. Lett.* **62** 2469
[35] Bastide J, Buzier M and Boué F 1988 *Polymer Motion in Dense Systems* ed D Richter and T Springer (Berlin: Springer) p 112
[36] Brochard F and de Gennes P G 1988 *C.R. Acad. Sci., Paris* II **306** 699